

Estimation of Mechanical Vibration Transmissibility due to Vibration Stress Effect on the Whole Body

Ajayi, S.T¹, Ogunsanya, A.O¹ and Aikhuele, D.O²

¹Department of Mechanical Engineering, College of Engineering, Bells University of Technology, Ota, Nigeria

¹Department of Biomedical Engineering, College of Engineering, Bells University of Technology, Ota, Nigeria

²Department of Mechanical Engineering, University of Port Harcourt, East-West Road, Port Harcourt, Nigeria.

*Corresponding author's email: danbishop_22@yahoo.co.uk

Abstract

Whole-body vibration exposure experienced in workstations on a daily basis have led to discomfort and health issues. Transmission of this type of vibration through the body segment can pose hazardous risks to the health and safety of the human body causing disorders and injuries. One of the conditions driving the transmission across regions of the body is the position of the human body. Therefore, this study was to develop a simple and reliable biomechanical model that can sufficiently optimized whole-body segments vibration transmissibility. A biomechanical model with six-degree of freedom lumped parameters was developed to study the response to whole-body segment vibrations. The model was designed using AutoCAD 2014 version, optimized using dynamic optimization on MATLAB version 2018. Anthropometry data with mean age of 39.75 ± 16.34 years were used in the estimation of stiffness and damping coefficient during the optimization process. Estimated values of transmissibility shows that the weight of the body segment, the stiffness constant, and the damping co-efficient affect the vibration frequency and the rate of transmissibility. The result revealed that the maximum transmissibility effect occurs within the lower limbs attaining a frequency range of 15 – 25 Hz while upper limbs experienced minimum effect in the range of 0 – 8 Hz. The vibration transmissibility transmitted during vertical posture attained the highest at 10 Hz. Vertical posture is less advantageous to the attenuation of vibrations conveyed to the human body, as a result, enhancing the impact acceleration frequency and intensifying the impacts that extend to other higher regions.

Keywords: Vibration, Biomechanical model, Transmissibility, Musculoskeletal disorders, Whole body, Vertical posture

Received: 9th May, 2023

Accepted: 30th August, 2023

1. Introduction

The body of a human is frequently subjected to vibrations in a variety of settings, including on-road vehicles like cars and buses and off-road vehicles like tractors and other heavy machinery. In each of these environments, through contact area human body gets vibrations that causes discomfort and health issues. Increased quantities of energy dissipated in form of vibration have shown to be transmitted to the human body causing adverse effects and injuries (Neil, 2005). In 2015, statistical analysis shows tremendous incident rate of musculoskeletal disorders of about 12.9% of workers fully engaged in their workstations in United States (Bureau of Labor, 2015). This vibration includes low frequency to high frequency vibration and their effect on the human body

depends upon the exposure time, the intensity of vibration, body posture, and body type and so on (Kumbhar, 2013). Intense low frequency of vibration (0.5 to 80 Hz) induced by unevenness of the surface and high-level vibration, reduce the level of comfort and increase the potential of musculoskeletal disorders (MSDs), particularly low back pain (LBP) (Burstrom *et al.*, 2014; Bovenzi *et al.*, 2006). Continuous exposure and increased magnitude of the vibration type causes poor concentration, fatigue, pain, and discomfort at the lower back and neck regions (Orelaja *et al.*, 2019).

The whole-body vibration that occurs due to the vibration transmitted is harmful to the health of the human body in workstation environment, and is a very important factor in workstation comfort. Assessment and exposure reduction in connection

with vibration exposure in workstation has been measured using experimental methods. The experimental methods have not been effective due to difference in each human body's sensitivity to vibrations. Therefore, the need to limit and eliminate this vibration types becomes imperative. It is on this premise that the vibration stress transmitted to the whole body (human body) is fully studied, analyzed, and evaluated. Over a decade, different artificial (biomechanical) models have been developed through varying test conditions like vibration excitation, human postural constraints and participant population (Behari and Noga, 2016). These models can be divided into three categories as lumped parameter, finite and multibody models (Bhagwan Kumbhar *et al.*, 2012; Kumbhar, 2013).

Two biomechanical models of seated position that studied the effects of human postures have been reported (Darling *et al.*, 2015; Gan *et al.*, 2015; Harsha *et al.*, 2014). Utilizing the model, analyze of low-frequency vibration environment in both horizontal (Darling *et al.*, 2015) and vertical stimulation directions (Gan *et al.*, 2015) were studied. Seven-DoF biomechanical model proposed by (Marzbanrad and Afkar, 2015; Afkar *et al.*, 2015; Marzbanrad and Afkar, 2013, Amir *et al.*, 2013) with the aid of unique variations shows better biomechanical responses of the human body (Marzbanrad and Afkar, 2013). The proposed model was used to evaluate and simulate health risks that were associated with different speeds passing through control humps (Afkar *et al.*, 2015; Marzbanrad and Afkar, 2015). Yanlong *et al.* (2016) studied Five-DoF vibration model of automobile ride comfort under vibration using pseudo-excitation method and stochastic road surface excitation as the main source of vehicle vibration. The ride comfort was analyzed using frequency-domain simulation. Deboli *et al.* (2017) and Prasad *et al.* (2014) analyzed the dynamic response of pneumatic seat installed on an old agricultural tractor. Different working surfaces at different tire pressure degrees, forward speeds and with or without a back seat were implemented in the analysis.

Pratik and Mangesh (2018) studied and analyzed the biodynamic response of car's seated human body moving at different speeds and different road surfaces. In another study by Javad *et al.* (2018), two biomechanical models to study vertical vibrations in the seated position with and without backrest support were also reported. Jamali Shakhilavi *et al.* (2018) proposed a six-DoF lumped-parameter model with six concentrated masses, connected using several linear springs and dampers.

The model was developed using ADAMS/CAR, utilizing the acceleration of the seat under various roads excitation for different amount of vehicle speeds. Jiang *et al.* (2020) designed six-DoF vibration isolation system with magneto-rheological damper (MRD) based on Stewart mechanism to reduce the mechanical vibration more effectively experienced by operators of the machine. Chougule and Naniwadekar (2019) studied the relationship between seat design and the vibrations transferred to the human body. The study covered literature on various dynamic parameters of seat cushions and suspensions, and the optimized methods of seat transmissibility. Singh *et al.* (2020) developed and validated with an experimental study by considering agricultural conditions on daily living, 3D CAD model with multi-layer solid modelling technique to predict human body response during exposure to vibrations. The CAD model possessed three layers with the vertical sitting position, and each layer defines the properties of human skin, muscles and bones.

Even though several researches regarding biomechanical model to analyze the effects of vibration transmissibility on the whole body have been proposed and reported, to the best of our knowledge, this is first biomechanical model to estimate the effect of vibration stress transmissibility on whole body during vertical posture. Hence, the aim of this study was to develop biomechanical model to study, analyze, and estimate the effect of whole-body vibration stress transmissibility during vertical posture. It is important to predict the risks of vibration exposure to the whole body in order to sufficiently minimize, control, or eliminate them and determine the optimal dynamic parameters in the early design to save time and money. The dynamic parameters like stiffness and damping coefficients of the human body were used in the optimization process.

2. Materials and methods

In this study, a six-DOF lumped parameter model was developed to study the response of vertical posture whole body vibrations as shown in Fig. 1. This is a linear six-DOF model in the 2D sagittal plane and composed of concentrated springs and masses linked together by dampers, and the vertical vibrations were transmitted to the whole body through the ground floor. Newtonian approach was used to derive the equation of motions (Bhagwan-Kumbhar *et al.*, 2012). Considering the dampers and springs links between the masses, linear equations governing this dynamic system's time-domain were applied (linear time invariant

system) and the differential equation has constant coefficients.

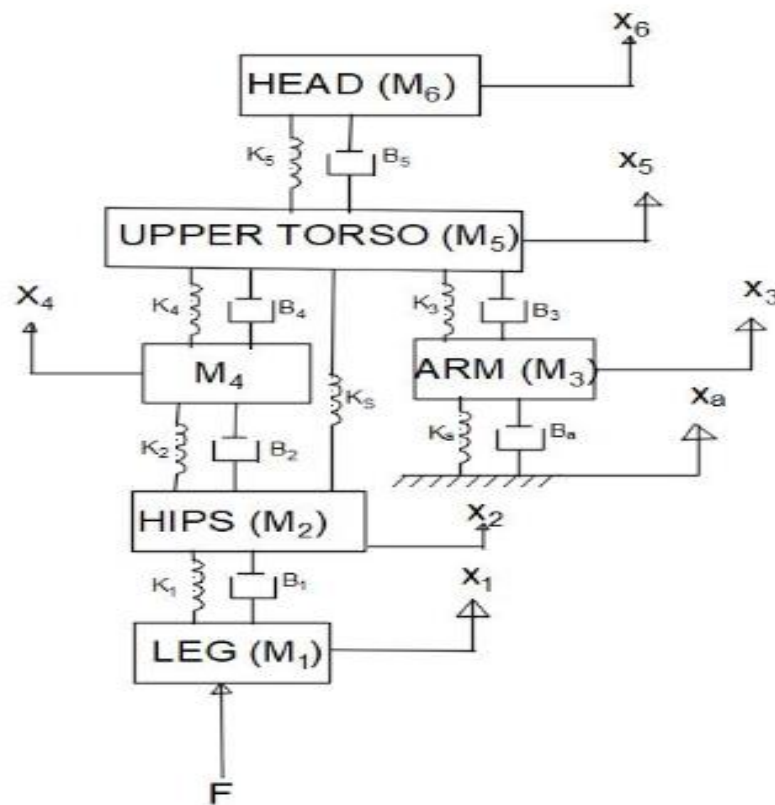


Fig. 1: Six-DoF biomechanical model vertical whole body

The human body has six body elements found in six different segments: Head and neck were considered as one segment (M_6) with a vertical spring having spring stiffness (K_5) and damping coefficient (B_5), the upper torso (M_5) with a spring stiffness (K_4), Abdomen (M_4) having spring stiffness (K_2), Arm (M_3) with a spring stiffness (K_3), Hips (M_2) with vertical spring stiffness (K_1), and the Leg (M_1) as shown in Figure 1. The equations of motion were rearranged to get mass, stiffness, damping and input

coefficient matrices. The matrices are useful for obtaining transmissibility functions. Using the free body diagram analysis, six-DoF biomechanical model equation of motion were derived using Newtonian method. The leg, M_1 gets input vibrations from floor, and were allowed to move in vertical posture. So, equation of motion of the mass, stiffness and damping coefficient are expressed as Equations (1) – (6).

$$F_1(t) = M_1 \frac{\partial^2 x_1}{\partial t^2} + K_1(x_1 - x_2) + B_1 \frac{\partial(x_1 - x_2)}{\partial t} \quad (1)$$

$$K_1(x_1 - x_2) + B_1 \frac{\partial(x_1 - x_2)}{\partial t} = K_2(x_2 - x_4) + B_2 \frac{\partial(x_2 - x_4)}{\partial t} + K_5(x_2 - x_5) + M_2 \frac{\partial^2 x_2}{\partial t^2} \quad (2)$$

$$K_2(x_2 - x_4) + B_2 \frac{\partial(x_2 - x_4)}{\partial t} = M_4 \frac{\partial^2 x_4}{\partial t^2} + K_4(x_4 - x_5) + B_4 \frac{\partial(x_4 - x_5)}{\partial t} \quad (3)$$

$$M_3 \frac{\partial^2 x_3}{\partial t^2} + K_3(x_3 - x_5) + B_3 \frac{\partial(x_3 - x_5)}{\partial t} = K_a(x_a - x_3) + B_a \frac{\partial(x_a - x_3)}{\partial t} \quad (4)$$

$$K_3(x_3 - x_5) + B_3 \frac{\partial(x_3 - x_5)}{\partial t} + K_4(x_4 - x_5) + B_4 \frac{\partial(x_4 - x_5)}{\partial t} + K_5(x_2 - x_5) = M_5 \frac{\partial^2 x_5}{\partial t^2} + K_5(x_5 - x_6) + B_5 \frac{\partial(x_5 - x_6)}{\partial t} \quad (5)$$

$$M_6 \frac{\partial^2 x_6}{\partial t^2} = K_5(x_5 - x_6) + B_5 \frac{\partial(x_5 - x_6)}{\partial t} \quad (6)$$

where x and t is the excitation and time taken respectively.

Taking the Laplace transform of Equations (1) – (6) gave the following equations:

$$F_1(S) = M_1S^2X_1(S) + K_1X_1(S) - K_1X_2(S) + B_1SX_1(S) - B_1SX_2(S) \tag{7}$$

$$\begin{aligned} K_1X_1(S) - K_1X_2(S) + B_1SX_1(S) - B_1SX_2(S) \\ = K_2X_2(S) - K_2X_4(S) + B_2SX_2(S) - B_2SX_4(S) + K_5SX_2(S) - K_5SX_5(S) \\ + M_2S^2X_2(S) \end{aligned} \tag{8}$$

$$K_2X_2(S) - K_2X_4(S) + B_2SX_2(S) - B_2SX_4(S) = M_4S^2X_4(S) + K_4X_4(S) - K_4X_5(S) + B_4SX_4(S) - B_4SX_5(S) \tag{9}$$

$$\begin{aligned} M_3S^2X_3(S) + K_3X_3(S) - K_3X_5(S) + B_3SX_3(S) - B_3SX_5(S) \\ = K_aX_a(S) - K_aX_3(S) + B_aSX_a(S) - B_aSX_3(S) \end{aligned} \tag{10}$$

$$\begin{aligned} K_3X_3(S) - K_3X_5(S) + B_3SX_3(S) - B_3SX_5(S) + K_4X_4(S) - K_4X_5(S) + B_4SX_4(S) - B_4SX_5(S) \\ + K_5X_2(S) - K_5X_5(S) \\ = M_5S^2X_5(S) + K_5X_5(S) - K_5X_6(S) + B_5SX_5(S) \\ - B_5SX_6(S) \end{aligned} \tag{11}$$

$$M_6S^2X_6(S) = K_5X_5(S) - K_5X_6(S) + B_5SX_5(S) - B_5SX_6(S) \tag{12}$$

where S and X is the Laplace Transform Coefficients.

The transfer function is the ratio of forced output response to input excitation that is relationship between input excitation and output response representing the dynamic response of the model (Kumbhar, 2013). Transfer function was used to study its relative magnitude and phase of the excitation, expressed as Equation (13).

$$\text{Transfer Function} = \frac{\text{Response Function}}{\text{Input Function}} \tag{13}$$

Transmissibility is a non-dimensional term employ by finding the modulus of the transfer function. The magnitude of the transfer function represents the transmissibility, expressed as Equation (14).

$$|H(f)| = [(Re[H(f)])^2 + (Im[H(f)])^2]^{1/2} \tag{14}$$

The transfer function was determined for all six body segments in given frequency range (0 – 25 Hz) using Equation 13 and also, the transmissibility values of the body in the given frequency range. Transmissibility plot were obtained for all six-body segment in vertical posture while analyzing its dynamic response (Kumbhar *et al.*, 2013). Independent controllable parameters affecting the biodynamic response of a vertical human model include: weight, height, age, body mass index (BMI) and the two levels of low and high selected as primary parameters for this study as shown in Table 1. The baseline characteristic was determined using the body mass index. Anthropometric measurement data (Pratik and Mangesh, 2018) was adopted for the estimation of Mass, Stiffness, and Damping Co-efficient of human body segments.

Table 1: Anthropometric data parameter levels selected for the study

S/N	Parameters	Levels	
		1 (Low)	2 (High)
1	Parameter 1 (Weight)	40 - 59kg	60 - 89kg
2	Parameter 2 (Height)	1.55 - 1.70m	1.73 - 1.80m
3	Parameter 3 (Age)	20 - 39yrs	40 - 60yrs
4	Parameter 4 (BMI)	16.96 - 23.24	25.10 - 30.80

On the basis of anthropometric data, the proportion of the total body weight were estimated for different body segments. The division of masses for the six-DoF model was determine for different body segments as follows:

- (Head + Neck) = 7.5 % of Total Body Mass
- Upper Torso = 4.21 % of Total Body Mass
- Thorax = 21.516 % of Total Body Mass
- Diaphragm = 3.11 % of Total Body Mass
- Abdomen = 23.776 % of Total Body Mass

- Thigh = 18.2 % of Total Body Mass

Computing the stiffness of various body segments, the ellipsoids was considered, and the ratio of the truncated length (d_i) to the original length (c_i) of the

ellipsoidal segment was defined as truncation factor, and the ellipsoids method was considered as shown in Fig. 2.

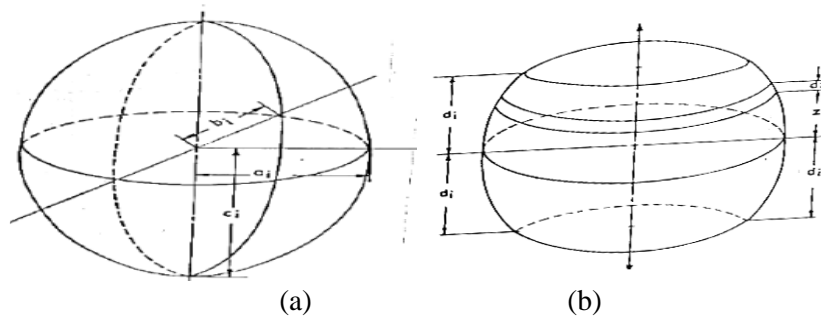


Fig. 2: Model stiffness computation using (a) semi ellipsoid Gupta (b) truncated ellipsoidal

Evaluating the segment's stiffness, the axial tension of a truncated ellipsoid was also considered. In the field of the assumptions regarding the mechanical properties and neglecting the strains due to the self-weight in comparison to those caused by the forces by the body, the expression of axial stiffness S_i , expressed as Equation 15.

$$S_i = \frac{\pi E a_i b_i}{c_i I_i} \text{ KN/m} \tag{15}$$

The modulus can then be expressed as Equation (16).

$$E = (E_b * E_t)^2 \tag{16}$$

where, E is the Modulus of elasticity of human body (13.06 MN/m²), E_b is the Elastic modulus of bone (22.6 GN/m²), E_t is the Elastic modulus of tissue (7.5 KN/m²), d_i is the Half length of the truncated ellipsoid. The moment of inertia of each of the ellipsoid segment can be expressed as Equation (17);

$$I_i = \log \left(\frac{(2 - tr')}{tr'} \right) \tag{17}$$

$tr = \frac{1-d_i}{c_i}$ refers to as the truncation factor, d_i is the half-length of the truncated ellipsoid. Ellipsoidal segment truncation of 5% at both ends that is d_i is the 0.95 c_i as proposed by (Singh et al., 2015; Nigam and Malik, 1987) was assumed; therefore, the segmental stiffness was determined by substituting $E = 13.06 \text{ MN/m}^2$ and solving Equation (7). Table 2 shows the semi ellipsoidal axes implemented in the study.

$$S_i = \frac{11164.277 a_i b_i}{c_i I_i} \text{ KN/m} \tag{18}$$

where S_i is the Stiffness of the segment (KN/m), E is the Modulus of elasticity of human body (13.06 MN/m²), a_i is the Semi-axis of the *major axis* of the tri-axial ellipsoid, b_i is the Semi-axis of the *median axis*, c_i is the original length of the ellipsoidal segment, I_i is the Moment of inertia of each ellipsoid segment, E_b is the Elastic modulus of bone (22.6 GN/m²), E_t is the Elastic modulus of tissue (7.5 KN/m²), d_i is the Half length of the truncated ellipsoid.

Table 2: Estimation of semi ellipsoid axes

Body Segment	Mass Element (kg)	Formulae		
		a_i	b_i	c_i
Head + Neck	M_6	$(L4/2) + (L5/2\pi)$	$(L4/2) + (L5/2\pi)$	$(L3/2) + ((L1-L2-L3)/2)$
Upper Torso	M_5	$(L9/2)$	$(L10/2)$	$(L8/2)$
Abdomen	M_4	$(L17/2)$	$(L18/2)$	$(L16/2)$
Arm	M_3	$(L22/2)$	$(L21/2)$	$(L20/2)$

Hips	M ₂	(L25/2)	(L24/2)	(L23/2)
Legs	M ₁	(L27/2)	(L28/2)	(L26/2)

Table 3: Standard damping ratio

S/N	Body Segment	Damping Constant, ξ_i
1	Head + Neck	0.009445
2	Upper Torso	0.3212
3	Abdomen	0.675
4	Arms	0.0055
5	Hip	0.75
6	Legs	1.25

In case of the damping constants, the standard damping ratio and designation proposed by (Zanwar et al., 2015) was used in this study as shown in Table 3. The damping ratio of the i^{th} segment can be expressed as; $K_a = 6,115 \text{ Nm}$, $K_s = 80,000 \text{ Nm}$ and $B_a = 100 \text{ N.s/m}$.

$$\beta_i = \xi_i * (S_i M_i)^{\frac{1}{2}} \tag{19}$$

where ξ_i is the Damping constant of the i^{th} segment (N-s/m), β_i is the Damping ratio of the i^{th} segment, S_i is the Stiffness of the segment (KN/m), M_i is the Mass of the segment, kg.

3. Results and discussion

In this study, a biomechanical model comprises of six-DoF lumped parameters was developed to study the response to whole-body segment vibrations. The human body response was estimated in vertical posture, the expressions of transfer

function were derived and the transmissibility values were evaluated. The characteristics of the whole-body model utilizing anthropometric data has the mean weight and the height of $62 \pm 20.22 \text{ kg}$ and $1.69 \pm 0.11 \text{ m}$ respectively and the baseline characteristic was $24.03 \pm 5.71 \text{ kg/m}^2$. Table 4 shows the weight distribution of the whole-body segment describe as the response of the body posture at the point of stimulation. Table 5 and Table 6 show the stiffness distribution and the damping element distribution of different segment of the whole-body model utilised in the model analysis and the optimization process, respectively. Transmissibility rate through the whole body was evaluated using the dynamic transfer function optimization technique, and the feet were considered to be fixed to the floor when vertical excitations is given at different frequency range of 0 Hz - 25 Hz (Phate et al., 2022).

Table 4: Weight distribution of different whole-body segment

Body Segment	M ₁	M ₂	M ₃	M ₄
	83kg	65kg	74kg	80kg
Leg	6.23	4.88	5.55	6.0
Hip	3.49	2.74	3.12	3.37
Arm	17.86	13.99	15.92	17.21
Abdomen	2.58	2.02	2.30	2.49
Upper Torso	19.73	15.45	17.59	19.02
Neck & Head	15.11	11.83	13.47	14.56

Table 5: Stiffness distribution of different whole-body segment

Body Segment	Male 1	Male 2	Male 3	Female 1
	83kg	65kg	74kg	80kg
Leg	162,320	138,529	156,603	150,393
Hip	162,021	158,700	157,777	152,985
Arm	26,787	29,556	31,014	33,179
Abdomen	17,329	17,159	22,247	21,851

Upper Torso	21,078	17,243	24,237	25,142
--------------------	--------	--------	--------	--------

Table 6: Damping element distribution by segments of the whole-body subject

Body Segment	Male 1 83kg	Male 2 65kg	Male 3 74kg	Female 1 80kg
Leg	132	116	124	130
Hip	4,579	4,052	4,323	4,495
Arm	36	32	34	36
Abdomen	36	32	34	36
Upper Torso	3,627	3,209	3,425	3,561
Neck & Head	9,238	8,176	8,724	9,070

Fig. 3 shows vibration transmissibility by varying the damping coefficient through the leg within frequency range of 0 – 16Hz. At this frequency, the body tissue was able to absorb the vibration energy. As the frequency of the vibration increases between 20 – 25Hz, the transmissibility rate increase causing transmission of vibration to other upper body segment. This indicates a high magnitude of acceleration of transmissibility in this body posture. Increased frequency results in the increase in transmissibility effect due to the vibration effect having the same frequency as the ground floor resulting from the reduced body mass and damping coefficients, thereby, damping the effect of the vibration. In addition, the increase in frequency was also due to low body mass of the body segment, thereby increasing the transmissibility rate to the upper body segment.

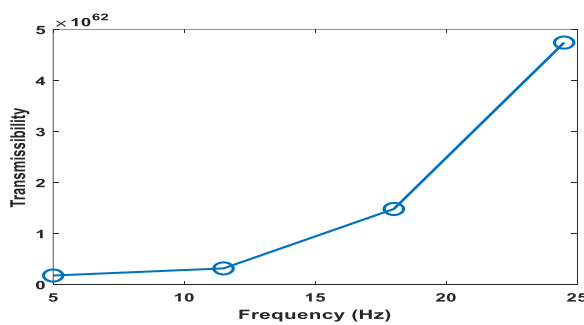


Fig. 3: Transmissibility of through the leg in vertical posture

Fig. 4 shows the transmissibility effect as the vibration frequency passes through the hip region of the body segment. The transfer function increases with increase in frequency due to low vertical damping that is the low body mass of the hip, the higher magnitudes of transfer functions and the peak in the frequency range. The magnitude of acceleration of transmissibility was reduce

compared to the leg transmissibility. This could be because of the effect of the shock-absorbing component of the hip. As the transmissibility passes through the ankle and knee by varying the damping co-efficient, the vibration energy is been absorbed by their components, sending up reduced value of the magnitude of acceleration. As soon as the transmissibility rate reaches some certain level with further increase in frequency (20 – 25 Hz) because the body tissues were unable to absorbed the effect of the vibration.

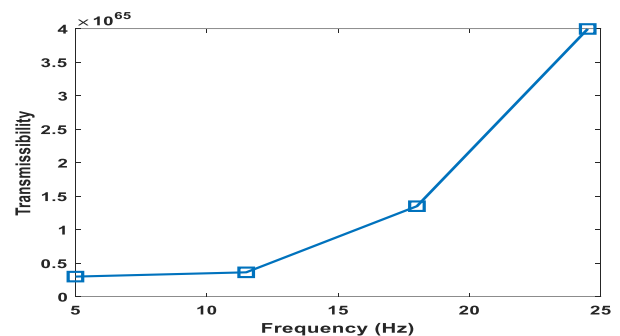


Fig. 4: Transmissibility through the hip in vertical posture

Fig. 5 shows that high stiffness and high damping coefficient increases transmissibility as frequency increases due to the damping effect at reduced body mass. As the transmissibility effect was transferred to the internal organs (Abdomen) with high damping and stiffness coefficient, and reduced body mass of the internal organs, the frequency at the transmissibility peak increases. The increased damping coefficient results in increased static compression of the surface. In addition, the magnitude of resistance increases in this body posture with respect to the contact surfaces. At a transmissibility of below 0.5 and frequency of 0 – 8 Hz, the resonance frequency is still the organ suspension resonances frequency. The increase in transmissibility rate could result in consistent beating of the organs such as the heart, lungs and so

on, against each other and the rib cage. The significant increase in transmissibility observed as frequency increases by varying the stiffness, the damping coefficients in this body position can be attributed to the high stiffness, and the high body mass within this body segments. The increase in frequency of vibration from 0 – 8 Hz indicate little or no effect of the damping on the transmissibility. As soon as the frequency exceeds 10 Hz, there was significant increase seen in transmissibility rate.

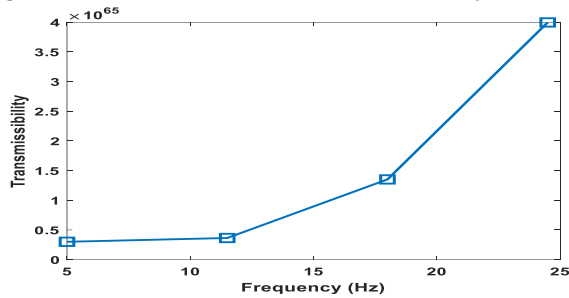


Fig. 5: Transmissibility through internal organ (abdomen) in the vertical posture

Fig. 6 shows that the higher damping coefficient and the higher body weight decreased transmissibility as frequency increases, reason been the presence of intervertebral disc within the upper torso acting as shock absorber and providing the vertical damping effect. The increased body weight increases the absorbing power, thereby decreasing the transmissibility rate as frequency increases. The damping efficient tends to damp the vibration's effect at higher estimated value. More so, the frequency of transmissibility peak value was reduced for this body posture, proven that the resonance frequency was reduced. The transfer function peak could be decreased by increasing the suspension damping. By selecting proper stiffness and damping coefficients, the excitation frequency can reduce the transmissibility at these frequencies to minimize the transmissibility to the other body segments and maximize comfort (Kumbhar, 2013).

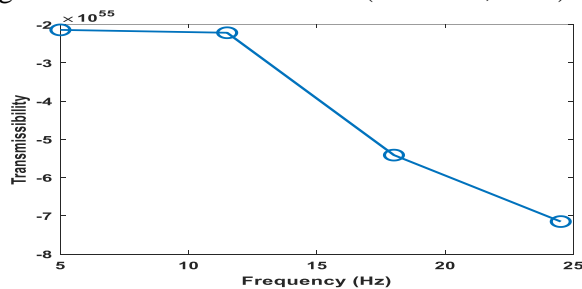


Fig. 6: Transmissibility through the upper torso in the vertical posture

Fig. 7 shows that as the magnitude of acceleration moved upward to the lower arm, transmissibility effect decreases with increased frequency. The low damping coefficient and high body mass initially shows little effect of the damping but with lower damping coefficient, the transmissibility effect increases with increased frequency. Lower damping and higher body mass coefficient reduced the transmissibility effect at the initial stage. Therefore, selecting proper stiffness and damping coefficient will allow minimum vibrations to be transferred to the other body segments. High damping effect and high body mass show decreased transmissibility, indicating effect of the damping coefficient on the transmissibility rate. The high damping coefficient shows negative value as the frequency increases. Further increase in frequency, significantly decrease the transmissibility. Compared to upper torso, transmissibility rate is reduced to minimum. Vibration transmissibility occurs within this body segment and subsequently, the acceleration of the magnitude to the neck and the head.

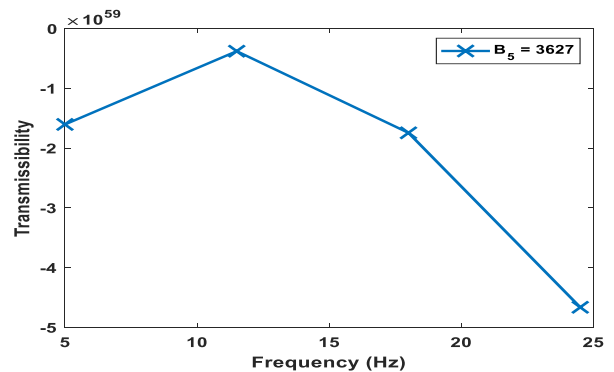


Fig. 7: Transmissibility through the arm in the vertical posture

Fig. 8 shows the variation in percentage increase of transmissibility revealing steady frequency between 0 to 5 Hz. Further increase was observed, maximum at 10 Hz as the frequency increases further but decreases within the frequency range of 10 to 15 Hz. In the frequency range between 15 to 20 Hz, percentage increase in transmissibility (0.4) was constant, and later increases within the frequency range of 20 to 25 Hz (Aisyah Adam et al., 2019). Table 7 shows the percentage increase in transmissibility and ratio of change of transmissibility during vertical posture.

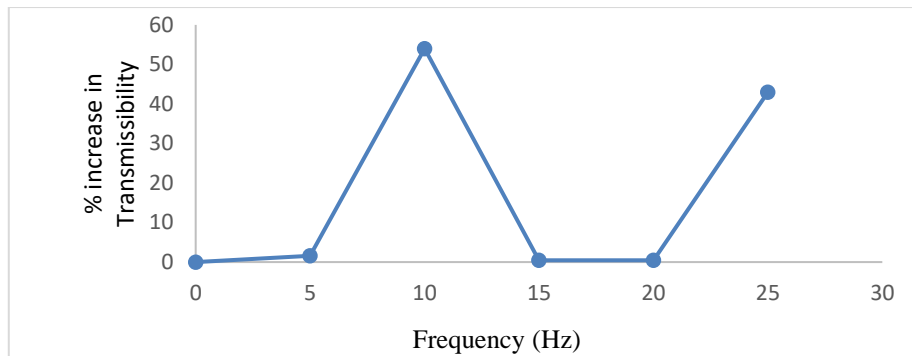


Fig. 8: Percentage increase in transmissibility of vibration

Table 7: Estimated rate of transmissibility, stiffness constant and percentage increase of the transmissibility

Rate of Transmissibility	Stiffness Constant	% Increase in Transmissibility	Ratio of Change of Transmissibility
126	151,961	1.57	$B_1 : B_2$ 1:35
4,362	157,871	54	$B_2 : B_3$ 125:1
35	30,134	0.44	$B_3 : B_4$ 1:1
35	19,647	0.44	$B_4 : B_5$ 1:99
3,456	21,925	43	

The responses of whole-body model under certain vibration (excitation) were studied in terms of transmissibility function in this study. In vertical posture, the excitation of the leg through floor surfaces are usually transmitted to the head through the entire body segment. The lower extremity's vibration transmissibility to the upper extremity is important to express the whole-body's vibration characteristics. The significant increase in the magnitude of acceleration of vibration observed in this body position suggests expressive non-interference of vibrations transmitted through the whole-body segments. This can be explained by the realignment of body segments and the consequent activation of the muscles involved in maintaining posture. The increased muscle activation promotes changes in musculoskeletal tissues' elastic and damping properties. Due to the vertical posture, there was increase in muscle tension, resulting in fatigue. With respect to vibration transmissibility through body segments, interpretation of the transfer function indicates higher transmissibility of the feet (leg) with low body mass and high damping coefficient. Due to the absorption of the excitation of the magnitude accelerated as the transmissibility moved up to other body segment like ankle and knee, suggesting effective attenuation of the vibratory stimuli, thus minimizing the magnitude of accelerations transmitted to the other body segments (Vasconcellos et al., 2014).

On the one hand, the absorption at hip region with high damping coefficient suggests that vibration's attenuation was high as the frequency of vibration increases (Table 7), suggesting high transmission of acceleration to the upper limbs. Although the body position exerts a major influence on the attenuation of vibrations, this interference occurs more isolated and more expressively at the first two moments of transmission. Because of the greater attenuation at leg and hip, the magnitude of vibration reaching the point of the lumbar spine was not as expressive as a result of the absorption of the vibration by intervertebral disc present within spine. Therefore, less susceptible to variation, meaning there were no longer many stimuli available for transfer to the head. The position's influence was more evident at the level of the hip. Above the hip, vibration was strongly attenuated by the internal organs. The lower limbs' action has been emphasized in this model; during whole body vibration, the muscles within the leg were the most participatory and the main muscles responsible for the attenuation of vibration are between the ankle and knee. Similarly, the thigh, quadriceps and hamstring muscles also contribute strongly to the damping or attenuation of vibration originating from the ground floor. Ankle and knee extension decreased the tension on the lower limbs' posterior muscles, with a negative impact that results in reduced attenuation. Lower activation of these

muscles as a result of knee and hip extension will permit a low intensified participation in the attenuation of vibrations, which continue to propagate after induction of the muscle, increasing the vibratory range and resulting in higher accelerations to the spine, arm, abdomen, upper torso, neck and head. In addition to increased transmissibility, body segments' realignment does not allow more stable position leading to unbalanced body posture. More so, the foot does not provide a large amount of proprioceptive information. Thus, the body proprioception was lower, with less efficient activation of the muscles necessary to attenuate acceleration of the transmissibility. This shows that the body posture adopted does not in any way increase the likelihood that resonance peak frequency will occur in the 15–25 Hz range by interfering with the propagation of vibration via regions of the body, allowing accelerations to reach the upper (Vasconcellos et al., 2014). The body posture is slightly affected by the resonance frequencies of vibration. Changes in the resonance frequency are apparent due to changes in stiffness and damping coefficient exhibited within the body segment (Aisyah Adam et al., 2019).

The present study employed six-DoF biodynamic model in 2D, coupled with six types of mass, spring stiffness and damper that assist in the selection of dynamic parameters. The equation of motion was derived for the coupled model. Transmissibility graphs were generated from an upright position after the transfer functions for impulses were computed. Based on the transmissibility results, the human body segment under isolation had the best performance. This study revealed most standing operators on daily basis are exposed to whole body vibration of high intensity. Also, the present study reveals that the vertical posture adopted does not interfere with vibration's transmissibility through the whole-body segments. Therefore, this position is less favorable to the attenuation of vibration transmissibility.

4. Conclusion

Model to predict and estimate human body response under whole-body vibration has been developed and optimized in the present study. The vibration transmissibility values in the present model segments suggested a high transmissibility rate within the leg and the hip. At the same time, abdomen and arm have the lowest value due to the damping factor that was effective in the vertebra column that tends to reduce the effect of vibration transmissibility. The findings of the study

demonstrate that the frequency as well as the body posture during a vertical operation are determining variables affecting how much vibration is propagated.

Conflicts of interest

The authors declare that they have no conflict of interest.

Funding

There is no fund to declare/not applicable

Informed consent

Informed consent was obtained from all individual participants included in the study.

References

- Afkar, A., Javanshir, I., Ahmadian, M.T. and Ahmadi, H. (2013) Optimization of a passenger occupied seat with suspension system exposed to vertical vibrations using genetic algorithms. *Journal of Vibroengineering*, 15(2):979–991.
- Aisyah-Adam, S., Abdul-Jalil, N. A., Razali, K.A.M. and Ng, Y.G. (2019) The effects of posture on suspension seat transmissibility during exposure to vertical whole-body vibration. *Journal of Physics: Conference Series*, 1262(1):012026.
- Bhagwan-Kumbhar, P., Xu, P. and Yang, J. (2012) A literature survey of biodynamic models for whole body vibration and vehicle ride comfort. Volume 6: 1st Biennial International Conference on Dynamics for Design; 14th International Conference on Advanced Vehicle Technologies, 671–687.
- Behari, N. and Noga, M. (2016) Vibration transmissibility behaviour of simple biodynamic models used in vehicle seat design. *Technical Transaction Mechanics*, 5M, 1–12.
- Bovenzi, M., Rui, F., Negro, C., D'Agostin, F., Angotzi, G., Bianchi, S., Bramanti, L., Festa, G., Gatti, S., Pinto, I., Rondina, L. and Stacchini, N. (2006) An epidemiological study of low back pain in professional drivers. *Journal of Sound and Vibration*, 298(3):514-539.
- Bureau of Labour Statistics (2015) The quest for meaningful and accurate occupational health and safety statistics. United State of America Monthly Labour Review (Retrieve 02-10-2022). <https://www.bls.gov/opub/mlr/2015/home.htm>.
- Burström, L., Nilsson, T. and Wahlström, J. (2015) Whole-body vibration and the risk of low back pain and sciatica: a systematic review and meta-analysis. *International Archives of Occupational and Environmental Health*, 88(4):403-418.

- Chougule, M.M. and Naniwadekar, A.M. (2019) Seat Transmissibility and Human Comfort – A Review. *International Research Journal of Engineering and Technology (IRJET)*, 6(12):1974–1976.
- Darling, J., Hillis, A.J. and Gan, Z. (2015) Development of a biodynamic model of a seated human body exposed to low frequency whole-body vibration. *Journal of Vibration Engineering Technology*, 3(3):301–314.
- Deboli, R., Calvo, A. and Preti, C. (2017) Whole-body vibration: measurement of horizontal and vertical transmissibility of an agricultural tractor seat. *International Journal of Industrial Ergon*, 58:69–78.
- Gupta, T.C. (2007) Identification and experimental validation of damping ratios of different human body segments through anthropometric vibratory model in standing posture. *Journal of Biomechanical Engineering*, 129(4):566–574.
- Harsha, S.P., Desta, M., Prashanth, A.S. and Saran, V.H. (2014) Measurement and bio-dynamic model development of seated human subjects exposed to low frequency vibration environment. *International Journal of Vehicle Noise and Vibration*, 10(1-2): 1-24.
- Jamali-Shakhlavi, S., Marzbanrad, J. and Tavooosi, V. (2018) Various vehicle speeds and road profiles effects on transmitted accelerations analysis to human body segments using vehicle and biomechanical models. *Cogent Engineering*, 5(1461529):1-17.
- Javad, M., Somaye, J. and Iman, T. A. (2018) Project: Biomechanical Modeling of a Seated Human Body Exposed to Vertical and Horizontal Vibrations Using Genetic Algorithms.
- Jiang, M., Rui, X., Zhu, W., Yang, F. and Zhang, J. (2020) Modeling and control of magnetorheological 6-DOF stewart platform based on multibody systems transfer matrix method. *Smart Materials & Structures*, 29(3):035029.
- Kumbhar, P.B. (2013). Simulation - Based Virtual Driver Fatigue Prediction and Determination of Optimal Vehicle Seat Dynamic Parameters. Texas Tech University.
- Kumbhar, P.B., Xu, P. and Yang, J. (2013) Evaluation of human body response for different vehicle seats using a mutibody biodynamic model. SAE Technical Paper 2013-01-0994, 1-14.
- Manojkumar, M. and Chougule, A.M.N. (2019) Seat Transmissibility and Human Comfort – A Review. *International Research Journal of Engineering and Technology*, 6:1974–1976.
- Marzbanrad, J. and Afkar, A. (2013) A biomechanical model as a seated human body for calculation of vertical vibration transmissibility using a genetic algorithm. *Journal of Mechanics in Medicine and Biology*, 13(04):1350053.
- Neil, J.M. (2005) Human response to vibration. New York Washington D C: Taylor & Francis e-library.
- Nigam, S.P. and Malik, M. (1987) A Study on a Vibratory Model of a Human Body. *Journal of Biomechanical Engineering*, 109(2):148–153.
- Orelaja, O.A., Wang, X., Ibrahim, D.S. and Sharif, U. (2019) Evaluation of health risk level of hand-arm and whole-body vibrations on the technical operators and equipment in a tobacco-producing company in Nigeria. *Journal of Healthcare Engineering*, 2019:1-12.
- Phate, M.R., Galkwad, P.P. and Toney, S.B. (2022) Analysis of seat to head transmissibility of the seated human body using artificial neural network. *Journal of the Institute of Engineers (India): Series C*, 103:557-571.
- Prasad, K., Xu, P. and James, Y. (2014) Optimal Seat Dynamic Parameters Determination for Minimizing Virtual Driver's Fatigue. SAE Technical Paper, 12.
- Pratik, P. and Mangesh, R. (2018) Phate exploring biodynamic response (apparent masses) of a seated human body exposed to external excitation in vertical direction. *International Journal of Industrial Engineering & Production Research*, 29:415–428.
- Singh, A., Singh, I. and Kalsi, S. (2020). Transmissibility evaluation of whole-body vibration using three-layer human CAD model. *Journal of The Institution of Engineers (India) Series C*, 101(3), 595–602.
- Singh, I., Nigam, S.P. and Saran, V.H. (2015) Modal analysis of human body vibration model for Indian subjects under sitting posture. *Ergonomics*, 58(7):1117–1132.
- Vasconcellos, R.P., Schütz, G.R. and dos Santos, S.G. (2014) The interference of body position with vibration transmission during training on a vibrating platform. *Brazilian Journal of Kinanthropometry and Human Performance*, 16(6):597–607.
- Yanlong, Z., Lixia, C., Li W. and Wenxue, Z. (2016) Vibration analysis of 5-DOF vehicle model under stochastic road surface excitation. *ICIEA*, 2016:1-4.

Zanwar, D.R., Deshpande, V.S., Modak, J.P., Gupta, M.M. and Agrawal, K.N. (2015) Determination of mass, damping coefficient, and stiffness of production system using convolution integral. *International Journal of Production Research*, 53(14):4351–4362.